DTIC

Finite Element Analysis of the Double Lap Joint with an Elastic-Plastic Adhesive

C. Pickthall, M. Heller and L.R.F. Rose

DSTO-TR-0528

DEPARTMENT OF DEFENCE

DEFENCE SCIENCE AND TECHNOLOGY ORGANISATION

Finite Element Analysis of the Double Lap Joint with an Elastic-Plastic Adhesive

C. Pickthall, M. Heller and L.R.F. Rose

Airframes and Engines Division
Aeronautical and Maritime Research Laboratory

DSTO-TR-0528

ABSTRACT

For an effective adhesively bonded reinforcement of a (typically cracked) plate, sufficient load must be transferred by the adhesive into the reinforcement to prevent the underlying damage from growing. Under severe load, the adhesive may yield plastically. Notwithstanding possible adhesive failure, this may be beneficial to the reinforcement by reducing the peak stress adjacent to the crack. In this paper, characterisation of this stress reduction compared to the (non-yielding) elastic case, was sought by examining the influences of configurational parameters including plate, adhesive and reinforcement moduli, and adhesive yield stress. Finite element (FE) analyses were conducted for a two-dimensional section through a double-sided (symmetric) lap joint, representative of a typical repair. Stress reductions in the reinforcement of the order of 25% were found. The adhesive yield was shown to be dominated by shear stress, and thus the adhesive behaved essentially one-dimensionally. The linear increase in plastic zone length with applied load, as predicted by the Hart-Smith one-dimensional theory, was in good agreement with the FE results. However the observed load transfer length was 6-18% longer than predicted.

DEPARTMENT OF DEFENCE

DEFENCE SCIENCE AND TECHNOLOGY ORGANISATION

Published by

DSTO Aeronautical and Maritime Research Laboratory
PO Box 4331
Melbourne Victoria 3001

Telephone: (03) 9626 7000
Fax: (03) 9626 7999

AR-010-216
May 1997

APPROVED FOR PUBLIC RELEASE

Finite Element Analysis of the Double Lap Joint with an Elastic-Plastic Adhesive

Executive Summary

At least three methods are available to restore serviceability of an aircraft with damage such as cracking in structural components and battle damage. These include replacing the damaged part, riveting or bolting on a reinforcement plate, and application of an adhesively bonded reinforcing patch over the damage. This third method features reduced downtime, and avoids further damage caused by drilling more holes. It requires that the reinforcement be stiff enough to take sufficient load to prevent the underlying damage (crack) from growing, but not so stiff that it substantially alters the stress distribution originally designed for in the structure. This work was undertaken to address two issues concerning bonded repair, the first being the accuracy of a RAAF engineering standard covering this type of repair. The second issue is the high level of stress in the reinforcement, and whether this can be reduced enough to eliminate possible failure of the reinforcement.

The RAAF engineering standard is based on a simple model. This paper seeks to establish a basis for the accuracy of the model, or to produce more accurate formulae. The focus is on a (symmetric) double-sided lap joint, representative of the worst-case repair of a through-cracked plate but without bending. There is a brief examination of one-sided repairs where peel stresses and bending are more important. Load transfer from plate to reinforcement occurs via (principally shear) stress in the adhesive. Finite element (FE) simulations using the PAFEC computer package produce the underlying data for analysis. With the symmetric lap joint, the dominant adhesive stress is found to be shear. This explains the accuracy of the one-dimensional model which only allows for longitudinal stresses in the plate and reinforcement, and shear in the adhesive.

This work extends the model to include the situation where the adhesive yields plastically. Above a specified (yield) stress, the adhesive distorts further without carrying any higher stress. Although this yielding is normally dependent on all the stress components, the dominance of shear meant the adhesive was again well described by a 1-dimensional model. This yielding extends the length over which the adhesive transfers load from the plate to the reinforcement. If the adhesive does not fail, this has the beneficial effect of lowering the peak stress occurring in the reinforcement adjacent to the crack. This reduction is significant: from around 1.6 times the average stress, to 1.3 times. Characterisation of this beneficial effect is sought by examining its dependence on configurational parameters including plate, adhesive and reinforcement moduli, and adhesive yield stress. The linear increase in plastic zone length with applied load, as predicted by the model, is closely simulated by the FE analysis although the observed load transfer length is 6-18% longer than calculated.

This work has shown that the simple model underlying the RAAF design standard on bonded repair accurately describes the behaviour of the repair components under load. The model was extended to allow for plastic yielding in the adhesive. This was shown to have the benefit of lowering the peak stress occurring in the reinforcement.

Authors

C. Pickthall
Airframes and Engines Division

Colin Pickthall completed a B. Sc. (Hons.) in Physics at Monash University in 1985, and completed his Ph.D. at Monash University in 1993. He commenced work in Materials Division at the (then named) Aeronautical Research Laboratory in 1991. His work has focussed on theoretical and analytical approaches in the areas of stress analysis and fracture mechanics, together with some finite element validation. He is currently a Research Scientist in the Airframes and Engines Division.

M. Heller
Airframes and Engines Division

Manfred Heller completed a B. Eng. (Hons.) in Aeronautical Engineering at the University of New South Wales in 1981. He was awarded a Department of Defence Postgraduate Cadetship in 1986, completing a PhD at Melbourne University in 1989. He commenced work in Structure Division at the Aeronautical Research Laboratory in 1982. He has an extensive publication record focussing on the areas of stress analysis, fracture mechanics, fatigue life extension methodologies and experimental validation. Since 1992 he has lead tasks which develop and evaluate techniques for extending the fatigue life of ADF aircraft components and provide specialised structural mechanics support to the ADF. He is currently a Senior Research Scientist in the Airframes and Engines Division.

L.R.F. Rose
Airframes and Engines Division

Francis Rose graduated with a B.Sc (Hons) from Sydney University in 1971 and a PhD from Sheffield University, UK in 1975. He was appointed as a Research Scientist at the Aeronautical Research Laboratory in 1976 and is currently the Research Leader in Fracture Mechanics in the Airframes and Engines Division. He has made important research contributions in fracture mechanics, non-destructive evaluation and applied mathematics. He is the regional Editor for the International Journal of Fracture and a member of the editorial board of Mechanics of Materials. He is also a Fellow of the Institute for Applied Mathematics and its Applications, UK and a Fellow of the Institution of Engineers, Australia.

Contents

1. Introduction

In the contexts of structural integrity and life extension, adhesively bonded (reinforcement) patches have been used to repair cracked metallic plates (Baker and Jones(1), Rose *et. al*(2)). For an effective repair, the adhesive must transfer sufficient load into the reinforcement, to prevent the underlying damage (crack) from growing. At the same time, the reinforcement should not be so stiff that it substantially alters the stress distribution originally designed for, in the structure.

In severe cases, the adhesive may yield plastically. If the adhesive does not actually fail, this plastic yielding may benefit the repair by lowering the peak stresses occurring in the reinforcement adjacent to the crack. However, it is desirable that the yielded zone be small enough to preclude subsequent adhesive degradation.

This work focusses on the double lap (symmetric) joint, as a model for two-sided repairs as indicated below. The aim is to seek design parameters that characterise the repair effectiveness, with greater accuracy than that obtained with the simple Hart-Smith(3) one-dimensional model.

Peel stresses and bending are known to be important in adhesive failure, particularly for a one-sided repair. These are briefly examined but are not the focus of this analysis. Reinforcements are usually tapered towards the edges to minimise these effects, but this may be restricted in situations where the patch size is limited.

In this work finite element analyses using the PAFEC level 8.1 package were conducted. These results were initially benchmarked against known analytical results for an elastic adhesive. They were then used to produce data for the case where the adhesive becomes plastic, yielding above a nominated von Mises (Henshell(4)) yield stress.

1.1 The Geometry of the Simplified Problem

The bonded-reinforcement repair of a crack is a three-dimensional problem, as shown in Figure 1. In the present analysis, a two-dimensional slice (**A-B** in Figure 1) is taken through the plate and reinforcements including the critical region in the vicinity of the crack. This models the repair as a double (symmetric) lap joint, representing the "worst case" repair where the crack extends right across the plate. In view of the symmetry either side of **A-B**, there is no displacement out of the **A-B** plane. This constrains the problem in Figure 1b to plane strain.

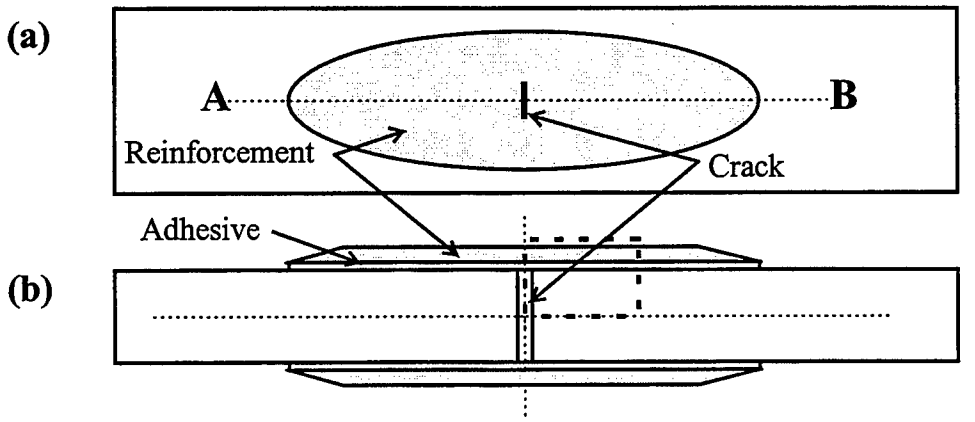

Figure 1. (a) A reinforcement patch repair and (b) the corresponding double lap joint with (symmetry) reduced region shown dashed.

Two further assumptions permit the reduction to a conceptually and analytically simpler problem shown by the dashed rectangle in Figure 1b.

1. The edge of the reinforcement and edge taper are far away compared to the load transfer length across the adhesive. This leads to a region far from the crack, and edge taper, of constant and equal strain ε_{xx} in the plate, adhesive and reinforcement. The problem can then be truncated, replacing the part to the right with uniform stresses across the plate, adhesive and reinforcement in proportion to their moduli.

2. Symmetry restricts the problem, to a region above the centre line and to the right of the crack with appropriate constraints as shown in Figure 2.

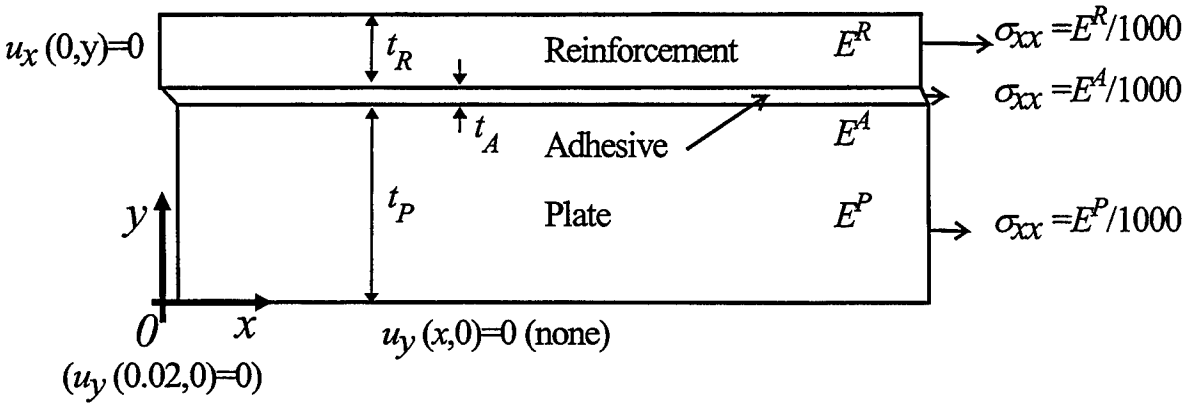

Figure 2. Reduced double lap joint problem showing the configurational parameters of thickness (t), Young's modulus (E) and constraints: displacement (u) and the applied stresses for the reference load (constraints for the one-sided repair in parentheses).

For this problem, the centre line (y=0) constraint is that the vertical displacement u_y=0. The constraints along x=0 are that the crack face (plate) has σ_{xx}=σ_{xy}=0 and the reinforcement u_x=0 along x=0. For the one-sided case, the u_y=0 constraint is eliminated. An additional constraint is then needed to fix the overall vertical displacement: say $u_y(0,0)$=0. To simplify specification of the $u_x(0,y)$=0 boundary condition across the reinforcement, the plate has been terminated at x=0.02mm in the unloaded state. This means the crack has a finite but small width at zero load.

The simplified problem with boundary conditions is illustrated in Figure 2. It is assigned a depth into the page of w=100mm. The stresses on the right end of the plate at the 100% reference load level (denoted by F_R) then convert to forces given for the plate by (Table 1): $F=\sigma.t^P.w$=22.4kN. The parameters chosen for the analysis are set out in Table 1. Note that t_P is the half-thickness of the plate shown in Figure 1.

Table 1. The parameters used in the analysis.

Parameter	Plate	Adhesive	Reinforcement
Material	Al 2024	FM 73	Boron fibre (10 ply) composite
Young's Modulus: E (GPa)	72.4	1.890	210
Poisson's Ratio: ν	0.33	0.35	0.30
Thickness: t (mm)	3.10	0.20	1.27
Depth: w (mm)	100	100	100
Relative stiffness: Et (mm MPa)	224	0.4	263
Stress applied at 100% load: σ (MPa)	72.4	1.890	210
Force at 100% (F_R): F (kN)	22.4	0.04	26.3
Shear modulus: μ (GPa)*	27.2	0.70	79.6
von Mises yield criterion: σ^Y (MPa)		low: 37.0 high: 64.1	

* The shear modulus is given by $\mu = \dfrac{E}{2(1+\nu)}$

1.2 Specific Cases examined

The following cases were examined:

1. An elastic calculation for the two-sided (symmetric) joint is the benchmark case.
2. An elastic calculation for the one-sided reduced lap joint problem extracted from cracked-plate configurations as indicated above, is compared to 1.
3. The two- sided joint is then examined for two different plastic yield stress cases.

4. The one-sided plastic case is presented with its higher peel stresses, important for failure in some real repairs.
5. Two-sided cases with varying plate, adhesive and reinforcement moduli are examined to determine the effects of plasticity in these differing circumstances.

2. Mathematical theory

2.1 Separation of von Mises Stress Components

There are a number of analytical formulae needed in this analysis. In particular, the von Mises yield condition (Henshell(4)) is based on the effective stress σ_e where:

$$2\sigma_e^2 = \left(\sigma_{xx} - \sigma_{yy}\right)^2 + \left(\sigma_{yy} - \sigma_{zz}\right)^2 + \left(\sigma_{zz} - \sigma_{xx}\right)^2 + 6\left(\sigma_{xy}^2 + \sigma_{yz}^2 + \sigma_{zx}^2\right). \tag{1}$$

This has been split into the major (one dimensional) component σ_{xy} and an additional component σ_a.

$$\sigma_e^2 = 3\left\{\sigma_a^2 + \sigma_{xy}^2\right\}. \tag{2}$$

Restricting the problem to plane strain, the following equations are obtained.

$$\begin{aligned} &\sigma_{xz} = \sigma_{yz} = 0, \quad \sigma_{zz} = \nu\left(\sigma_{xx} + \sigma_{yy}\right) \\ &\sigma_a^2 = \frac{1}{3}\left\{\left[1 - \nu + \nu^2\right]\left(\sigma_{xx} - \sigma_{yy}\right)^2 + \left[1 - 2\nu\right]^2 \sigma_{xx}\sigma_{yy}\right\} \end{aligned} \tag{3}$$

Substituting in the value for FM73 adhesive, ν=0.35, this reduces to

$$\sigma_a^2 = \frac{1}{6}\left\{1.545\left(\sigma_{xx} - \sigma_{yy}\right)^2 + 0.18\sigma_{xx}\sigma_{yy}\right\}. \tag{4}$$

2.2 Load Transfer Length and Yield Load: One Dimensional Model

The Hart-Smith(3) one-dimensional model allows for longitudinal stresses only in the plate and reinforcement, and shear in the adhesive. By considering equilibrium of these forces acting on the components (Figure 3a), equations may be obtained for the stresses shown. The adhesive stress, $\sigma_{xy}^A(x)$ is found to decay exponentially with the form $\exp(-\beta x)$. The load transfer length, β^{-1}, is given in this model by

$$\beta^{-1} = \sqrt{\frac{E^P t_P}{\mu^A / t_A}}\sqrt{\frac{S}{1+S}} \quad \text{where the stiffness ratio is } S = \frac{E^R t_R}{E^P t_P}. \tag{5}$$

Here, R and P refer to the reinforcement and plate respectively.

This Hart-Smith model predicts a linear increase in plastic zone length with applied load. This can be seen in the following figure showing the σ_{xy} stress in the adhesive (the only stress considered in the adhesive in this model) after some plastic yield with the plastic zone length l_p. The total force transmitted across the adhesive (Figure 3b) is given by the area under the curve,

$$F_{\text{Trans}} = w \times \left[l_p \times \sigma^Y_{xy} + \int_{l_p}^{\infty} \sigma^Y_{xy} \exp(-\beta[x - l_p])\, \mathrm{d}x \right] = w \times E^P t_P \times \frac{F/F_R}{1000}. \qquad (6)$$

The 1000 arises because the reference load (F_R) is defined as that loading where the applied stresses are 1/1000 of the Young's modulus for the plate, adhesive and reinforcement respectively (Figure 2). As the applied load (F) increases, the plastic zone (l_p) must extend enough (Δl_p) to transmit the additional load. This will be proportional to $\Delta l_p \times \sigma^Y_{xy}$. For a one dimensional analysis, the von Mises yield criterion (equation (3) with σ_a=0), gives $\sigma^Y_{xy} = \sigma^Y/\sqrt{3}$.

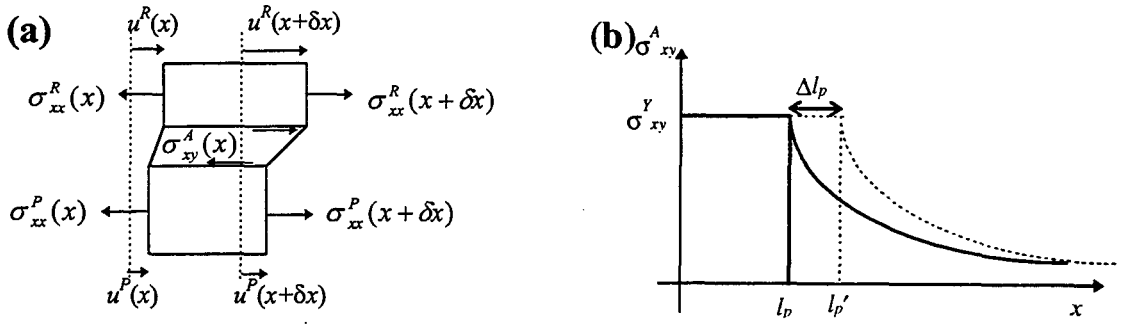

Figure 3. (a) Infinitesimal element used in deriving the one dimensional theory, showing the stresses and displacements considered. (b) Plastic zone of length l_p with exponential tail in the adhesive shear stress.

It is straight forward to carry out the intergation in equation (6) and rearrange to show the predicted linear increase in plastic zone length with applied load:

$$l_p = \frac{E^P t_P}{\sigma^Y_{xy}} \times \frac{F/F_R}{1000} - \frac{1}{\beta} = \frac{1}{\beta}\left(\frac{F}{F_Y} - 1\right). \qquad (7)$$

The second equality above introduces the load F_Y needed to initiate plastic yielding. The first shows that the plastic zone growth rate is only dependent on the plate properties and the adhesive yield stress.

3. Numerical Analysis

3.1 The finite element mesh

The mesh used in the PAFEC analysis is presented in Figure 4. The focus is on the critical region above the crack in the reduced configuration shown in Figure 2. Mesh refinement in this region is necessary due to the high stress gradients there. Optimisation of the angles used in the refinements and the choice of total mesh length (37mm) are discussed in appendix 0. Appendix 0 includes a listing of the PAFEC data file used in the initial plastic case. The 0.02mm offset of the left most nodes in the plate relative to those in the reinforcement, was discussed earlier with reference to the $u_x(0,y)=0$ boundary condition across the reinforcement.

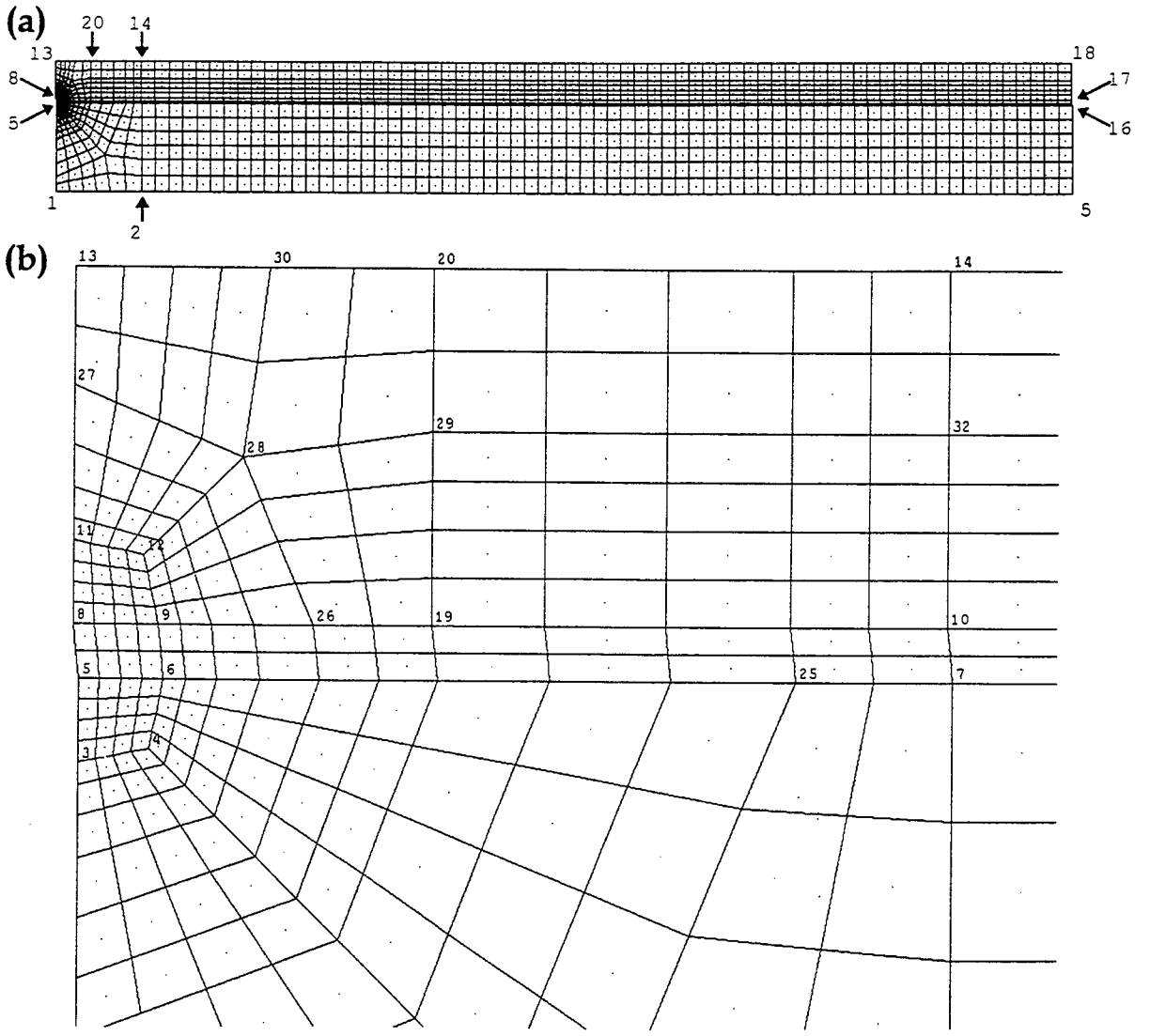

Figure 4. Mesh used in the PAFEC analysis. (a) Whole mesh of length 37mm. (b) Detail near the refinement.

3.2 Benchmark: Two-sided Elastic Case

The FE analysis required an initial elastic calculation before each plastic run to ascertain the load initiating plasticity. The plastic run then started just below this and increments took the load into the plastic regime. Each elastic case was run at the reference load F_R (Figure 2): an example is shown in Figure 5 with the (elastic) load scaled up to 220% of F_R, the same as the maximum load applied in the corresponding plastic case. The stresses of particular interest are σ_{xx} in the reinforcement along the top surface and the reinforcement-adhesive interface, and σ_{xy} in the adhesive, also along the interface. The stress components contributing to the von Mises stress, equations (2) and (4), are also presented.

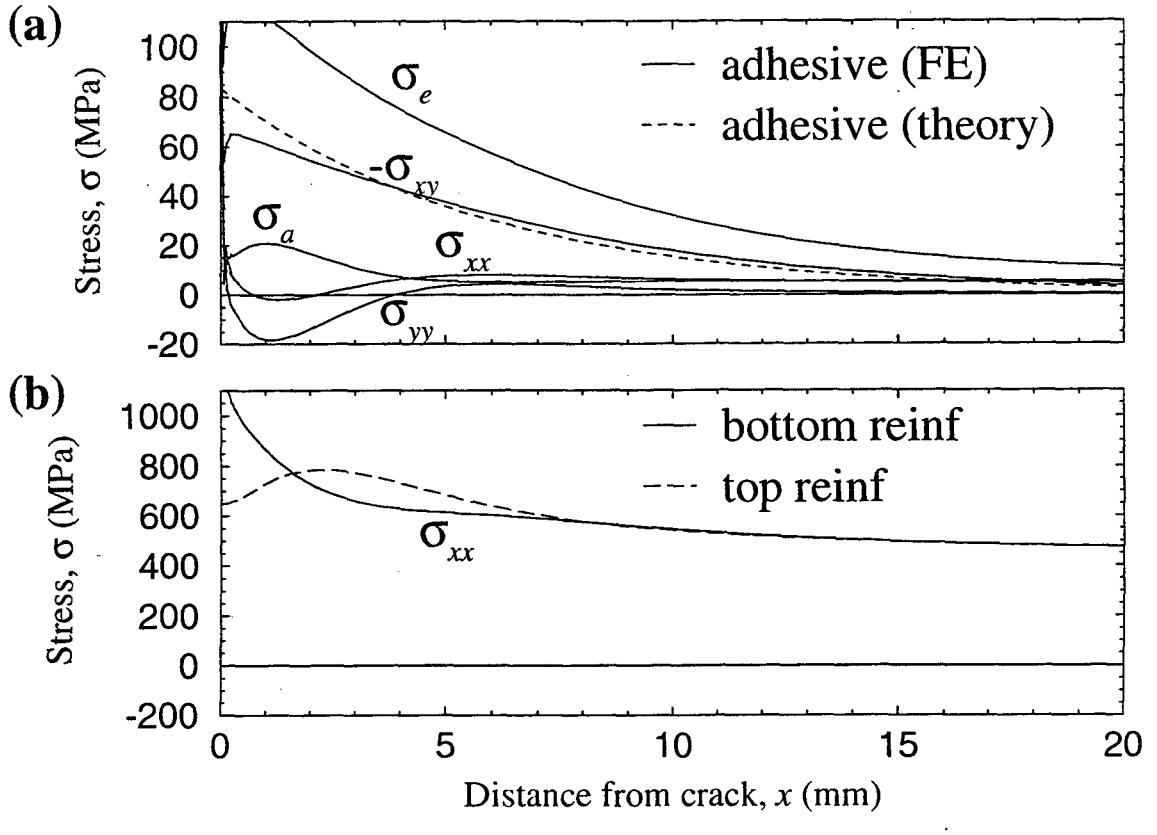

Figure 5. The finite element stresses calculated for an elastic adhesive at a load of 220% F_R.

In most cases, as demonstrated in appendix C, the elastic cases gave results broadly in line with the one dimensional theory for load transfer lengths.

3.3 Two-sided Plastic Cases

Two cases were examined with bi-linear adhesive stress-strain responses (Figure 6). The post-yield incremental moduli were $E \fallingdotseq E/10$ and $E \fallingdotseq E/100$ respectively. These

produced very similar results so that "elastic - perfectly plastic" was taken to be represented by the $E \leftarrow E/100$ results. There was only a small difference in these two cases when the growth of the plastic zone length against applied load (F/F_R) was plotted in Figure 9. The following figures present the data from calculations for the two-sided (symmetric) joint case. The stresses of particular interest include σ_{xx} in the reinforcement, both adjacent to the adhesive (nodes 8-17) and on the top surface (13-18), as well as σ_{xy} in the adhesive. The von Mises stress and its decomposition according to equation (3) are also plotted in Figure 7.

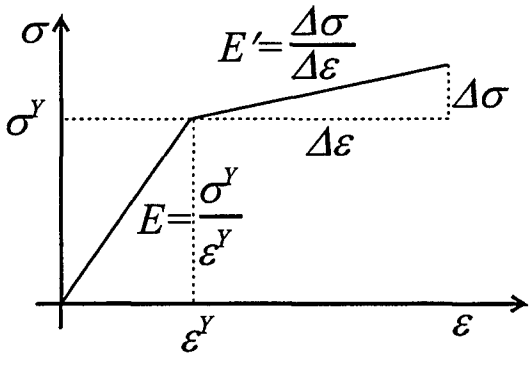

Figure 6. Elastic-plastic stress behaviour showing Young's modulus E and the post-yield modulus E'.

In this case, the smallness of the additional stress component σ_a, indicates that the dominant stress governing adhesive yield is σ_{xy}. This explains the accuracy of the one-dimensional model (3): the adhesive is yielding essentially one-dimensionally. The σ_{xx} stress along the reinforcement surface is interesting because it is measurable in a real specimen using strain gauges while the adhesive and reinforcement stresses along the adhesive line are not. If the behaviours at the top and bottom of the reinforcement and in the adhesive can be correlated, the onset or extent of plasticity may be ascertained easily in practice. The reinforcement surface stress peaks away from directly above the crack in the plate because there is always some bending of the reinforcement at this point. This bending towards the crack causes a lower (tensile) stress at the surface directly above the crack. The other stresses in the adhesive, σ_{xx} and σ_{yy}, are relatively small.

3.4 One-Sided Elastic and Plastic Cases

These cases were undertaken to investigate the magnitude of the peel stresses due to bending. They used the same mesh as the earlier calculations, and were derived by replacing the $u_y(x,0)=0$ constraint in Figure 2 by u_y $(0.02,0)=0$. They therefore correspond to one-sided repairs of plates half as thick as for the two-sided repairs. As shown in Figure 8, the stress σ_{yy} in the adhesive is much larger than in the two-sided case.

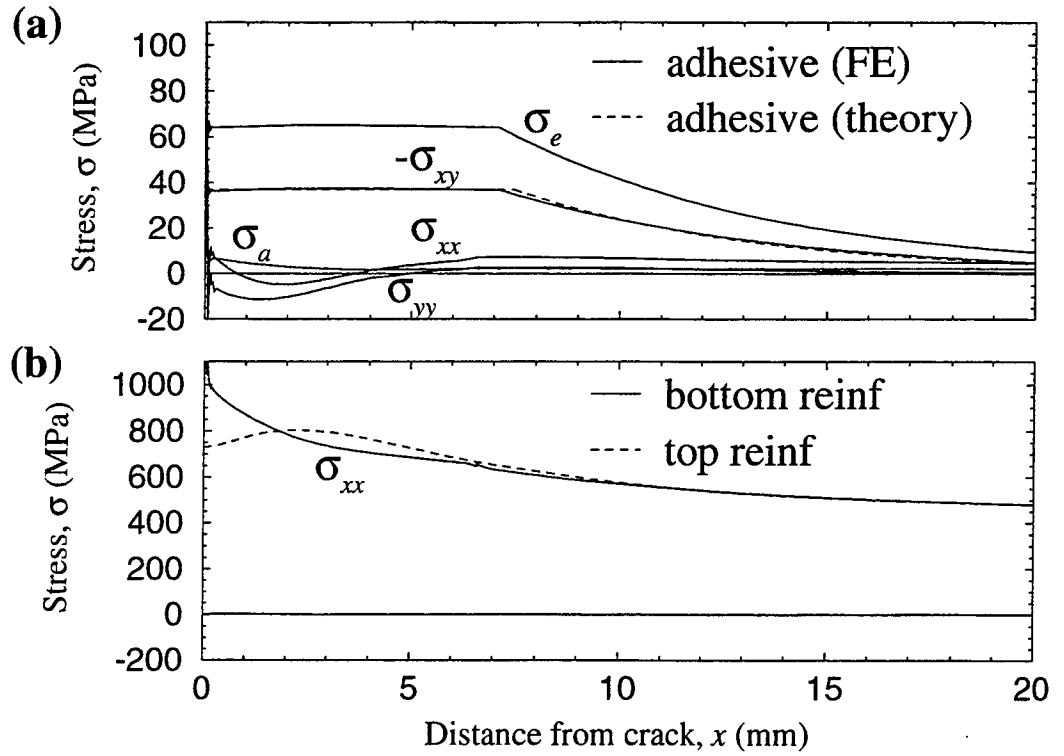

Figure 7. Finite element calculated stresses for the two-sided plastic case with an applied load of 220% F_R and post-yield modulus E'=E/100.

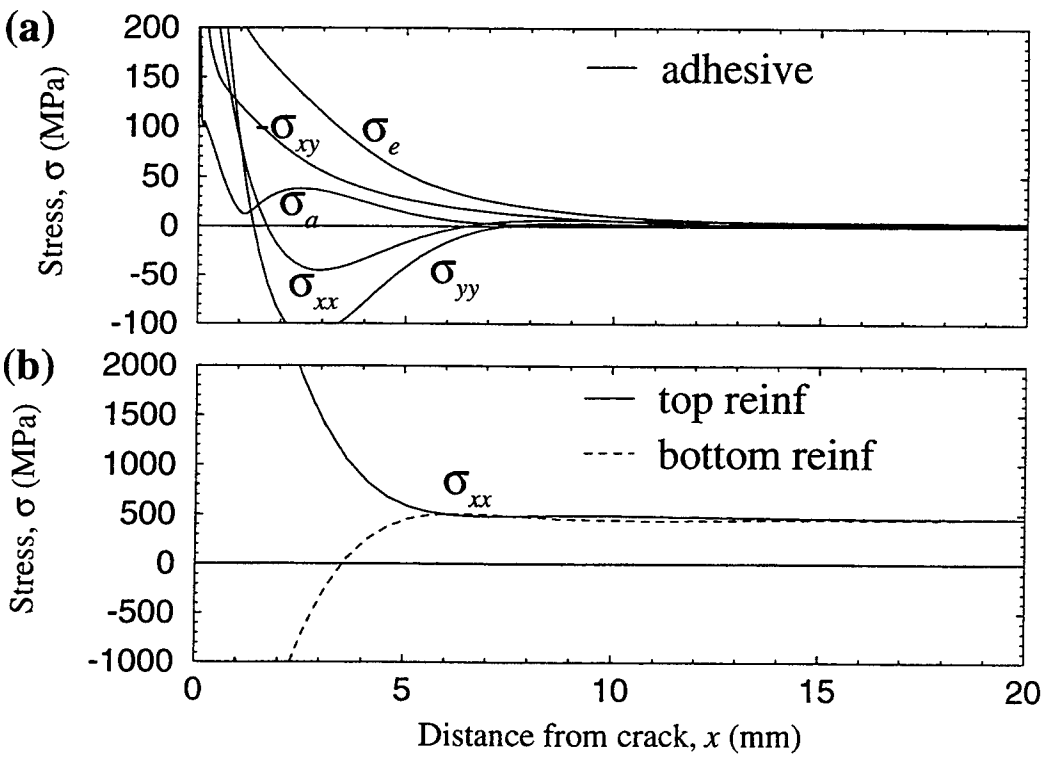

Figure 8. Stresses in the one-sided elastic case. The applied load is again 220% F_R.

The high stresses in the adhesive suggested that plastic yielding would occur at much lower loads than for the two-sided case. This was found as plastic yield would first occur here at only 4% F_R, compared to the 104% previously. To perform the plastic calculations, the increments were reduced from 10% load to 3% to ensure convergence at each load increment. The load was taken up to 40% only. Clearly, the von Mises stress decomposition indicates a large contribution by non-shear stresses. This case needs further investigation and is of interest because in practice bending can occur, and often only a one-sided repair is possible.

3.5 Discussion of Results to Date

The above calculations lead to several useful derived quantities, in particular the growth of plastic zone with increasing load. The one dimensional model leads to a linear relationship as indicated earlier in Figure 3. The growth in plastic zone length with applied load is shown in Figure 9 for the cases examined. The gradient of the line fits that predicted by the one dimensional model very well in the two-sided cases. This reinforces the earlier suggestion that the model is accurate because the dominant stress in the adhesive is σ_{xy}. For the one-sided case, plastic yielding commences at a much lower stress level and spreads faster due to the effect of the peel stress contributing to the von Mises yield criterion.

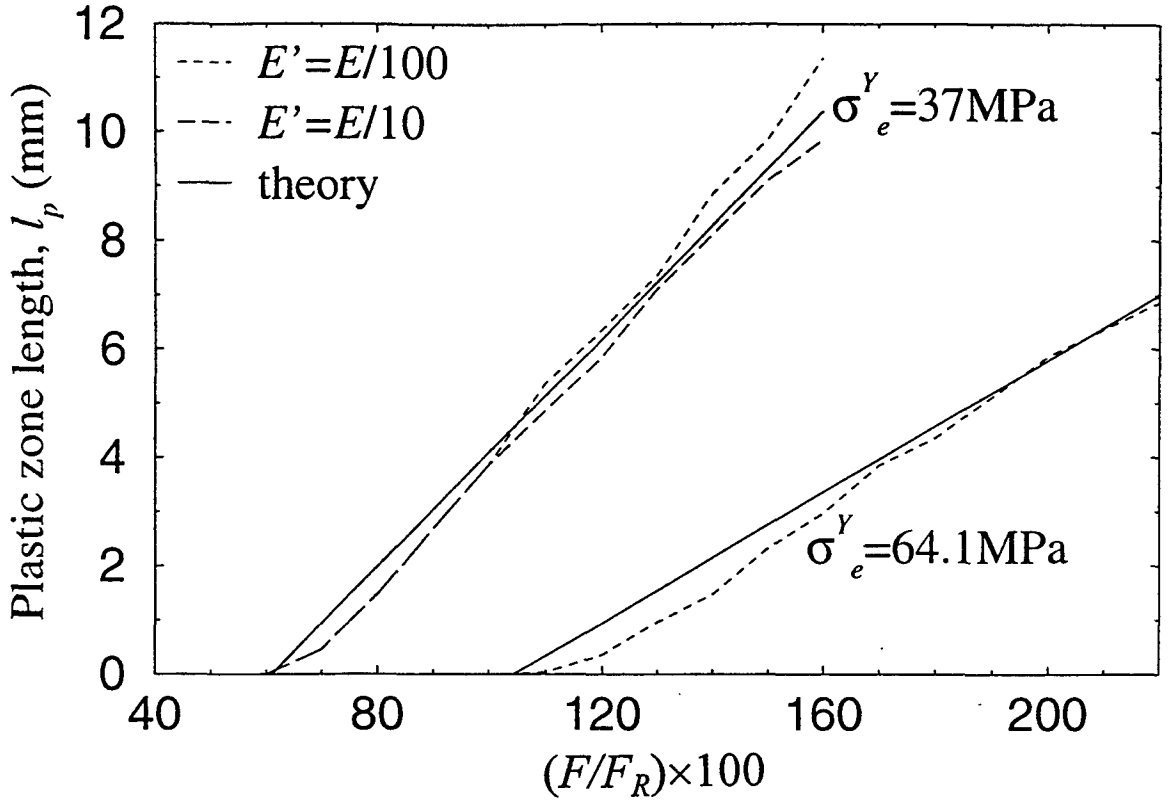

Figure 9. Plastic zone length growth with applied load.

While the plastic zone should not extend for a large proportion of the reinforcement length, its presence has the desirable effect of lowering the peak stress in the reinforcement. This is because adhesive yield reduces the load being transferred into the reinforcement at that point. Transference of this load occurs over a longer section of reinforcement than it would have without plasticity. The σ_{xx} stress distribution across the reinforcement is thus more uniform and not so concentrated next to the adhesive. This is particularly relevant above the crack in the plate. This stress relief may be shown (Figure 10) in two ways as follows.

1. The first method is by plotting the σ_{xx} stress across the reinforcement at x=0 (above the crack).
2. Plotting the normalised peak stress against normalised load provides a more graphic illustration. The normalised peak stress is that in the reinforcement just above the crack, divided by the average stress across the reinforcement along x=0. The normalised load is the current load relative to that needed to initiate plastic yielding.

Figure 10b shows a significant lowering of the normalised peak stress in the reinforcement, from 1.6 down to 1.2 at 220% F_R. This reduction may be an important factor in the choice of adhesive for this type of repair. The adhesive thickness and stiffness will also affect the stress concentration. Calculations with either a thinner or stiffer adhesive layer produced higher peak stress values.

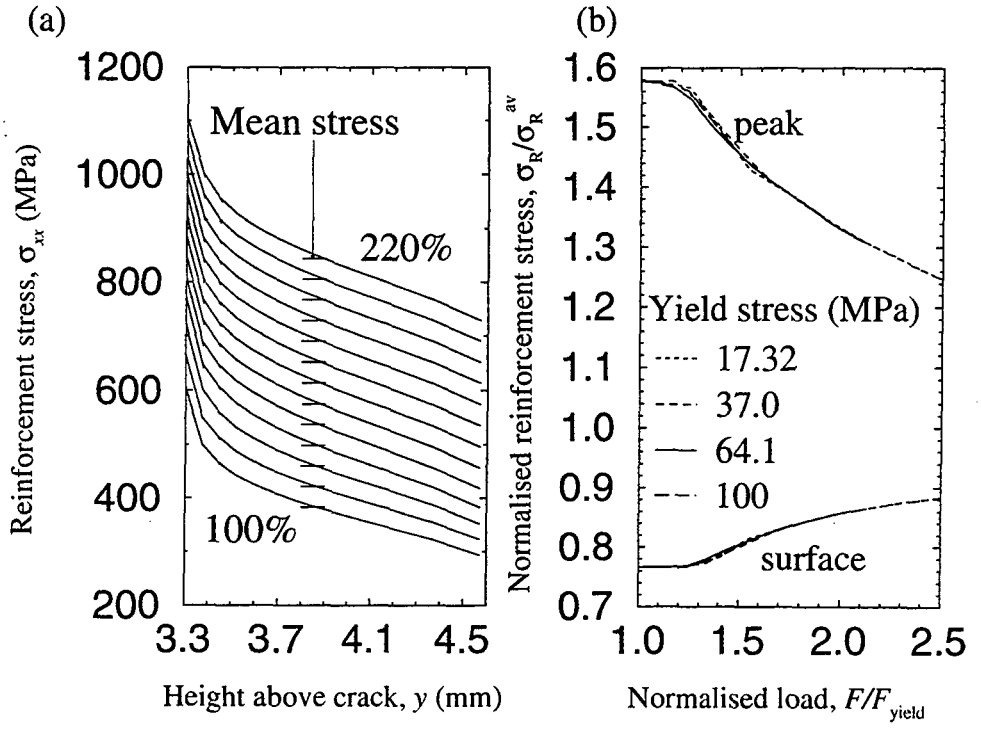

Figure 10. Stress relief through plastic yielding. (a) The σ_{xx} stress across the reinforcement at x=0 for increasing loads. (b) Normalised peak stress and surface stress against normalised load.

4. Configuration Variations

So far, this investigation has focussed on a single repair configuration, with the various thicknesses and moduli chosen being those of representative repairs. This section examines the effects of varying these parameters. In particular, the load transfer lengths obtained vary consistently with the (engineering) calculated values from equation (5) when the various moduli are varied. The actual values calculated using; (a) the formula, (b) those fitted to the exponential decay of the shear stress, and (c) those derived from the growth in plastic zone with applied load, are compared in Figure 11.

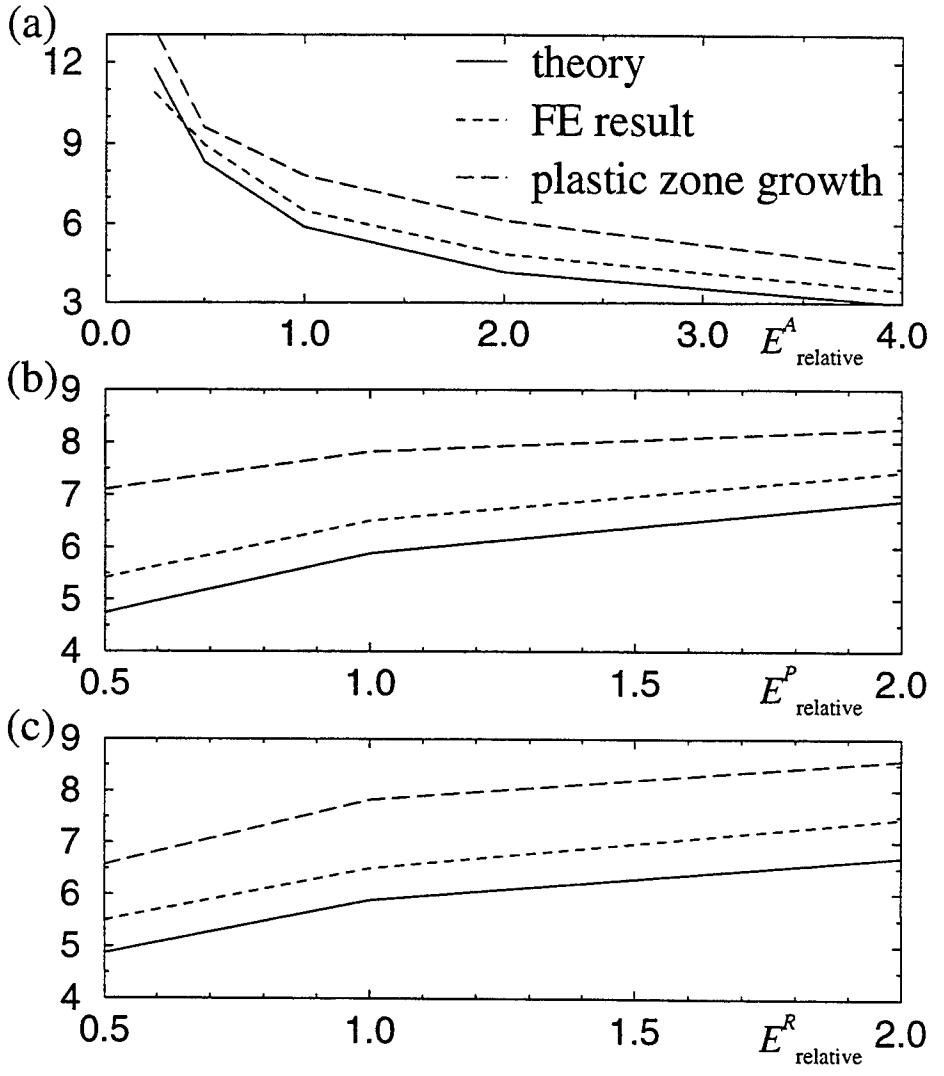

Figure 11. Variation in load transfer length, β^{-1}, for varying moduli of (a) adhesive, (b) plate, and (c) reinforcement. In each case, the modulus is expressed relative to that given in Table 1. For example, $E^A{}_{relative}=E^A/(1.890\text{GPa})$.

The load transfer lengths from the exponential decay and fitted to the plastic zone growth, agree qualitatively with the calculated values in their behaviour with variations in the moduli. Quantitative agreement among the three values is poor. Table 2 compares the load transfer lengths for the initial case.

Table 2. Comparison between values for the load transfer length as determined by the three methods, for the initial two-sided case.

Method of determination	Value (mm)
Calculated by equation (5)	5.881
FE result from stress decay	6.50
Fitted to plastic zone growth	7.82

The stress concentration above the crack, in the elastic case prior to plastic yield, also depends on the configuration. This is illustrated in Figure 12.

4.1 Plastic Zone Length: Growth with Applied Load

As indicated earlier, a longer plastic zone may be beneficial as it leads to a reduced stress concentration in the reinforcement above the crack. The zone should not be so long that it extends for a large proportion of the overlap, or else the joint is liable to failure. The one-dimensional model predicts that this behaviour is linear with applied load, and for the initial case shown in Figure 13, this is closely followed by the FE results.

Finding a configuration-independent behaviour for this plastic zone growth is desirable. To this end, the one dimensional model suggests that plotting plastic zone length normalised by the load transfer length, against load normalised by the yield load, should lead to a "universal plot". This was indeed the case for varying the adhesive yield stress, and was followed fairly well for the other cases except for the stiffer adhesive moduli (Figure 14). The problem with the $4E^A$ case in particular, seems to be a delay in the growth of the plastic zone with applied load above the initial yield load. It is not clear why this is so, but the subsequent growth rate agrees well with the theory.

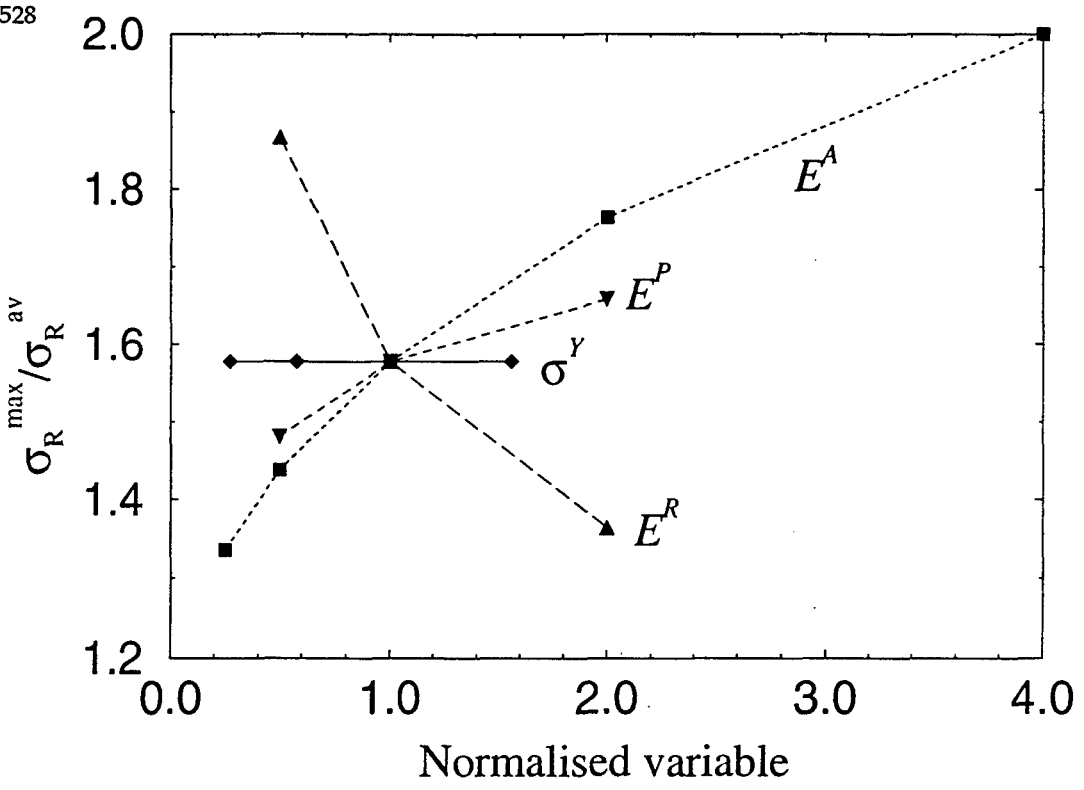

Figure 12. Variation in stress concentration above the crack with configurational parameters, in elastic cases. The "normalised variable" label refers to the scaling of each variable relative to its value given in Table 1.

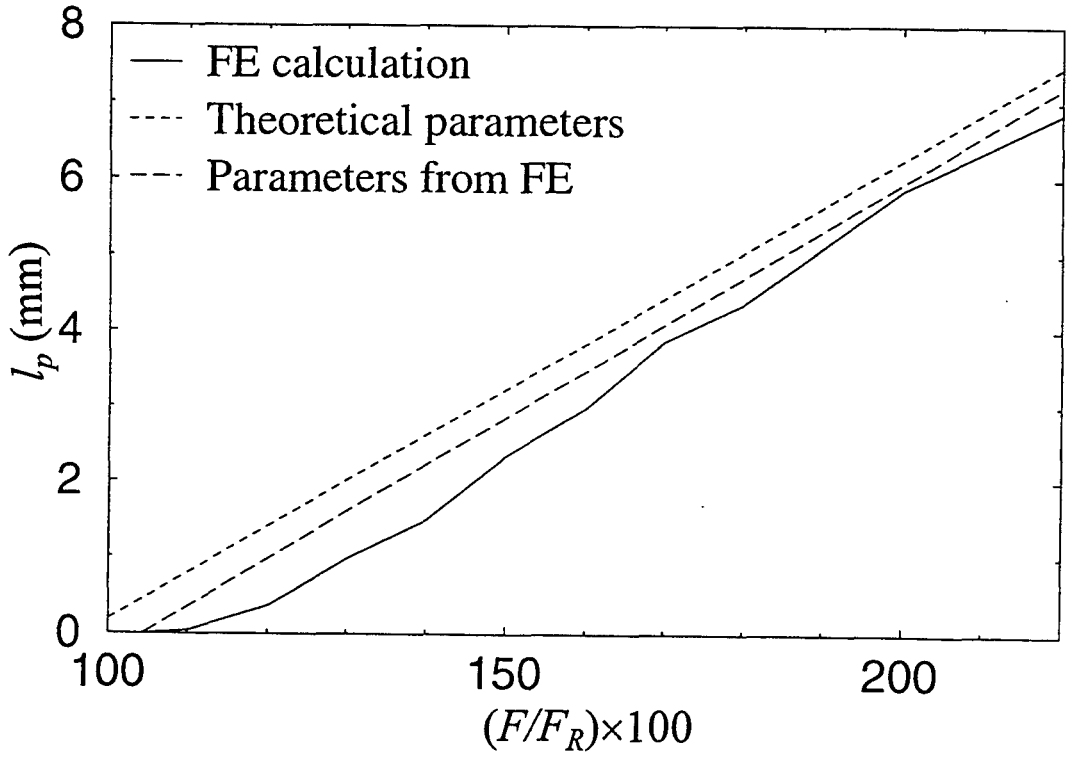

Figure 13. Growth in plastic zone length with applied load. Finite element results compared with the one dimensional model.

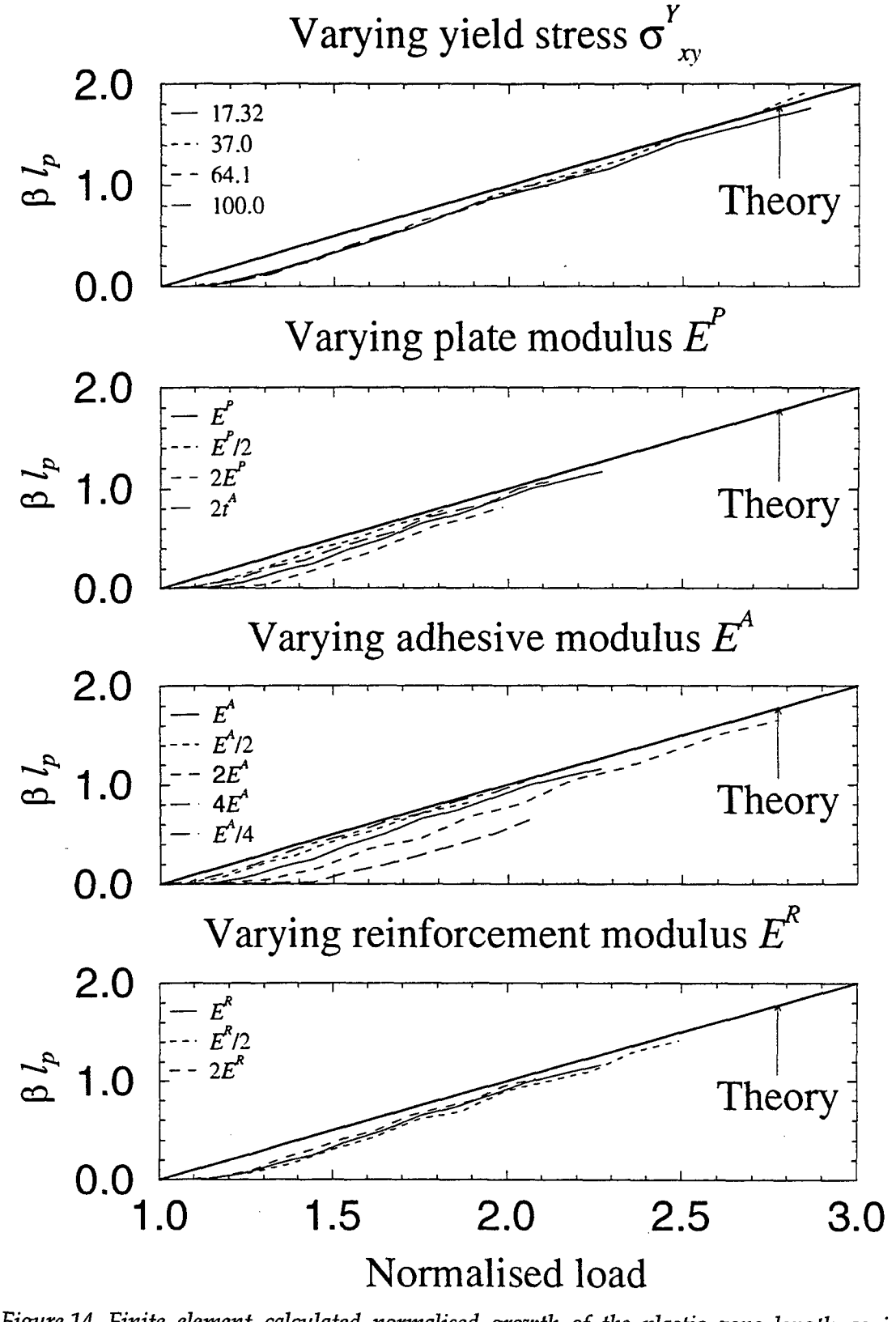

Figure 14. Finite element calculated normalised growth of the plastic zone length against normalised load for the various configurational parameters, showing behaviour fairly close to theory in most cases.

5. Conclusion

Stress reductions in the reinforcement near the crack region of the order of 25% (see for example Figure 10b) were obtained through plastic yielding of the adhesive. In the two-sided repair case, this yielding was dominated by shear stress, σ_{xy}, explaining the success of the Hart-Smith one-dimensional theory. The theoretical linear increase in plastic zone length with applied load was in good agreement with the FE results. However the observed load transfer length was 6-18% longer than that predicted by the theory.

6. References

1. **BAKER, A.A. and JONES, R.,** *Bonded Repair of Aircraft Structures,* 1988, Martinus Nyhoff Publishers, Dordrecht

2. **ROSE, L.R.F., CALLINAN, R.J., BAKER, A.A., SANDERSON, S. and WILSON, E.S.,** *Design Validation for a Bonded Composite Repair to the F111 Lower Wing Skin,* 1995, PICAST2-AAC6 Conference, Melbourne, March 20-23

3. **HART-SMITH, L.J.,** *Adhesive-Bonded Double-Lap Joints, Technical Report,* 1973, NASA CR 112235

4. **HENSHELL, R.D.,** *PAFEC 75 Theory, Results,* 1975, Nottingham University

Appendix A: Refinements to the Mesh

The mesh for the PAFEC routines uses 8-point quadrilateral elements, PAFEC type 36210. These preferably have near-equal side lengths and angles near 90°. The number of elements required is high due to the thinness relative to length of the adhesive layer that has two elements across the thickness. Halving the dimensions of all elements thereby quadrupling the total number of elements and leading to four across the adhesive, led to results insignificantly different to those using the mesh as presented.

A.1. Element angles

The simple method of obtaining mesh refinement near a point of interest, yields angles of 45° and 135° as shown in Figure 15a. This can be modified as shown in Figure 15b by constraining the points *A* and *B* to lie on the 45° line and varying angles *a*, *d* and *e*. Examining the location of point *A* first, its location fixes angle *a*. Angles *b* and *c* are then determined respectively as 270°-2*a* and 45°-*a*. Ideally all three angles would be 90° but this is not possible. The best option is to minimise their deviations from that by minimising

$$z = 2(a-90)^2 + (b-90)^2 + 2(c-90)^2. \qquad (8)$$

The weightings arise because there are two angles *a* and *c*. The result is *a*=78.8°, *b*=123.8° and *c*=112.4°.

A similar two-variable procedure was carried out with angles *d* and *e* leading to *d*=87.4°, *e*=71.5° and *f*=135°-*e*=63.5°. A preferred approach was to set *e*=*f*=67.5° so that the other three angles at *B* could be set equal at 75° and *d*=82.5°.

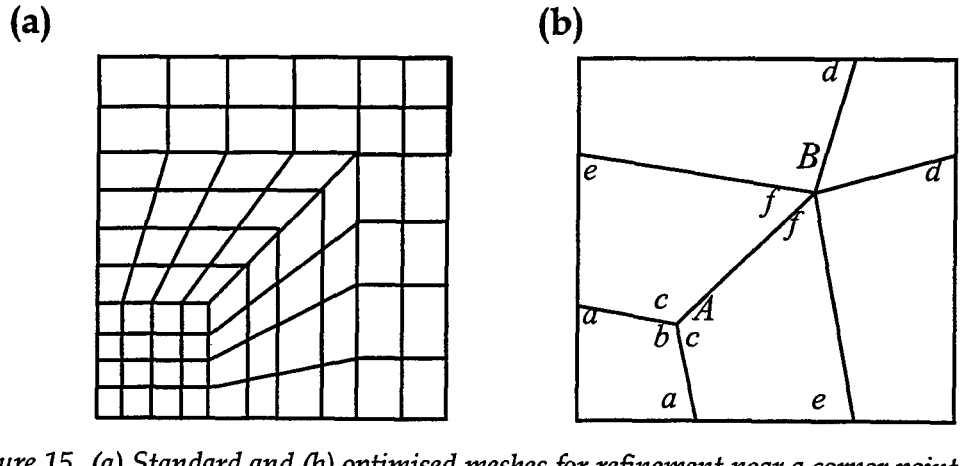

Figure 15. (a) Standard and (b) optimised meshes for refinement near a corner point. In (b), the mesh has been omitted for clarity.

A.2. Mesh length

The original length of the mesh was 20mm. With a load transfer length around 6.5mm however, the edge was affecting the results as indicated by very different load transfer lengths obtained for the elastic and elastic-plastic cases. Extension to 37mm by doubling the length (and number of elements) between nodes 2 and 15 brought these load transfer lengths into agreement.

A.3. Load increments

For the plastic calculations, PAFEC begins with a run using an applied stress below that needed to cause plastic yield. This stress was calculated from the earlier elastic run. The load is then incremented into plasticity. The increments must be small enough to allow convergence and accuracy at each step. With the von Mises yield criterion at σ^Y=37MPa, an initial elastic calculation indicated first plastic yield at 62% applied load. For plasticity, load increments of 5%, from 60% to 90% produced excellent agreement with the results using 10% increments. The latter were thus taken to be sufficiently accurate and increments calculated up to 160% load. Using the higher yield criterion of σ^Y=64.1MPa, first yield occurred at 104%. Plastic calculations commenced from an initial 100% load up to 220%, again in 10% increments.
In the one-sided lap joint, 10% increments led to irregularities in the stress plots. These were eliminated using 3% increments, but computing limitations restricted the number of increments to about 12. Initial plastic yield was also much lower, under 10% load. This case was therefore not loaded to high levels (maximum around 50%) and further investigation was suspended.

Appendix B: PAFEC Data File for the Base (Plastic) Case

The following data file listing is for the base case with plastic yielding at the von Mises yield criterion of σ^Y=64.1MPa. The parameters obtained in this case are shown in bold in Appendix C.

```
C
C DATA FOR - 2D PLANE STRESS BONDED LAP JOINT SPECIMEN
C OPTIMISED MESH AROUND END WITH BREAK IN PLATE
C BASE CASE, VON MISES=64.1MPA
C
CONTROL
FULL.CONTROL
TOLERANCE=10E-4
PLANE.STRAIN
PLASTIC
C C.SLOPE=-(FRACT OF E) TO APPROACH STRESS-STRAIN:
C 0= INIT STRAIN (MOVE HORIZONTAL), INF= INIT STRESS
C (MOVE VERTICALLY DOWN)
C C.SLOPE=
PHASE=1
PHASE=2
C PHASE=3
PHASE=4
C PHASE=5
PHASE=6
PHASE=7
C PHASE=8
PHASE=9
C NON.LINEAR.TOLERANCE=1 (1%= DEF)
BASE=4000000
C PHASE=10
C PIGS.STRESS.FILE
STOP
CONTROL.END
C
NODES
C NODE.NUMBER  AXIS.NUMBER X Y Z THICKNESS
NODE.NUMBER    X           Y
C PLATE NODES
C THE PLATE
1              0.02        0
2              3.12        0
3              0.02        2.8
4              0.27        2.85
C BETWEEN PLATE AND ADHESIVE
5              0.02        3.1
6              0.32        3.1
7              3.12        3.1
C BETWEEN ADHESIVE AND PATCH
8              0           3.3
9              0.3         3.3
10             3.1         3.3
C PATCH BODY AND TOP SURFACE
11             0           3.6
12             0.25        3.55
13             0           4.57
14             3.1         4.57
C POINTS AT X=INFINITY
15             37.12       0
16             37.12       3.1
17             37.1        3.3
18             37.1        4.57
19             1.27        3.3
20             1.27        4.57
C VARIABLE NODES TO OPTIMISE ANGLES
C NODE         X           Y
C IN PLATE (13,14,1,3,15)
C 21 0.4281+ 0.8683*T      0
C 22      0.02             3.1- 1.4142*T
C 23    0.02+ T            3.1- T
C 24      3.02             2.7050- 0.8683*T
C 25 0.02+ 1.4142*T        3.1
C IN PATCH (7,16,8,17,18)
C 26    1.4142*T           3.3
C 27       0               3.3+ 1.4142*T
C 28       T               3.3+ T
C 29      1.27             3.4672+ 0.8683*T
C 30 0.1672+ 0.8683*T      4.57
C SUB-DIVISIONS OF BLOCKS 9,11,12
C Y(31)= Y(24), Y(32)= Y(29)= Y(33)
C WITH T= 1.8
21             1.99        0
22             0.02        0.55
23             1.82        1.3
24             3.12        1.13
25             2.56        3.1
C WITH T= 0.6
26             0.85        3.3
27             0           4.15
28             0.6         3.9
29             1.27        3.99
30             0.69        4.57
C BLOCKS 9,11,12 SIB-DIVISIONS
31             37.12       1.13
32             3.1         3.99
33             37.1        3.99
C FOR STRESS IN ADHESIVE END
34             37.115      3.150
35             37.110      3.200
36             37.105      3.250
C END NODES
C
PAFBLOCKS
C BLOCK.NUMBER TYPE GROUP.NUMBER ELEMENT.TYPE PROPERTIES
C N1 N2 N3 N4 N5 TOPOLOGY
C REFERS TO MATERIAL AND PLATES AND MESH BELOW
C PROPERTIES=11
TYPE=1
ELEMENT.TYPE=36210
C
C N1=X-AXIS, N2 Y-AXIS TO DISCRETISE UNDER MESH
C(REFERENCE) BL,BR,TL,TR,BC,LC,RC,TC:
C B=BOTTOM,L=LEFT,R=RIGHT,T=TOP,C=CENTRE
C IN PLATE, 1=LEFT, 2=ADJACENT ADHESIVE, 3=TO RIGHT
BLOCK. GROUP. PROPERTIES N1 N2 TOPOLOGY
1     7     11          1  10 22,23,3,4
2     7     11          1  3  3,4,5,6
3     7     11          2  3  4,23,6,25
C ADHESIVE, 4=LEFT, 5=NEXT
4     3     12          1  4  5,6,8,9
5     3     12          13 4  6,7,9,10
```

```
C PATCH, 6=LEFT ADJACENT, 7=NEXT, 8=ABOVE
6     6     13        1  3  8,9,11,12
7     6     13        8  3  9,26,12,28
8     6     13        1  8  11,12,27,28
C FOR X=INFINITY TO RIGHT
9     7     11        6  3  24,31,7,16
10    3     12        6  4  7,16,10,17
11    6     13        6  3  10,17,32,33
12    6     13        9  3  19,10,29,32
C EXTRA FOR OPTIMISED ANGLES
C PLATE
13    7     11        1  5  1,21,22,23
14    7     11       14  5  21,2,23,24
15    7     11       14  3  23,24,25,7
C PATCH
16    6     13       15  3  26,19,28,29
17    6     13        1  5  27,28,13,30
18    6     13       15  5  28,29,30,20
C SUB-DIVISIONS OF BLOCKS 9,12,11= 19,20,21
19    7     11        6  5  2,15,24,31
20    6     13        9  5  29,32,20,14
21    6     13        6  5  32,33,14,18
C END PAFBLOCKS
C
MESH
C SINGLE DIGIT = NO. OF INTERVALS, LIST=RATIO
REFERENCE SPACING.LIST
C X LEFT END (1,2,4,6,8, 13,17) NOTE (BLOCK)
1         4
C X(3), INCLUDED WITH 14 IN MESH 13
2         8,11,15,21,21,21,40,43,44
C IN PLATE Y(2,3,15) AND PATCH Y(6,7,13) INCLUDE
C +5 IN 11,12
3         4
C IN ADHESIVE Y(4,5,10)
4         2
C IN PLATE Y(13,14) AND PATCH Y(17,18) INCLUDE
C +3 IN 11,12
5         2
C X TO INFINITY X(9,10,11,19,21)
6         68
C X TO INFINITY X(10), EXTRA OVER MESH 6 AS ADHESIVE THIN
C ********UNUSED NOW
7         34
C EXTRA BLOCKS 7,8
C X(7) AND Y(8), INCLUDED IN MESH 13
8         8,11,15,21
C X(12) FILL-IN PATCH BLOCK
9         40,43,44,28,28
C REVERSE OF MESH 2 FOR X(1)
10        44,43,40,21,21,21,15,11,8
C Y(9) INCLUDES MESHES 5,3 *******UNUSED NOW, Y(9)= MESH
C (3)
11        56,56,49,49,49,49
C Y(11,12) INCLUDES MESHES 3,5 ********UNUSED NOW, =MESH
C (3)
12        17,17,17,17,29,29
C X(5) INCLUDES MESHES (2,14) AND (8,15,9)
13        8,11,15,21,21,21,40,43,44,28,28
C PLATE X(14,15), INCLUDED IN MESH 13
14        2
C PATCH X(16,18), INCLUDED IN MESH 13
15        21,21
C END MESH
C
MATERIAL
C MATERIAL.NUMBER E NU RO ALPHA MU K SH BULK.M
C UNITS OF MPa AND mm
MATERIAL.NUMBER  E      NU
11               72400 0.33
C MU= (E/2)/ (1+nu)= 700 MPa FROM PETER CHALKLEY FM 73
C AT ROOM T
12                1890 0.35
13              207000 0.30
C END MATERIAL
C
PLATES.AND.SHELLS
C PLATE.NUMBER MATERIAL.NUMBER THICKNESS FACING.MATERIAL
C OUTER.LAYER.THICKNESS
C   RAD1 RAD2 (LAST 5 COLUMNS FOR SANDWICH CONSTRUCTION)
PLATE MATERIAL.NUMBER THICKNESS
11    11              100
12    12              100
13    13              100
C END PLATES.AND.SHELLS
C
RESTRAINTS
C NODE.NUMBER PLANE AXIS.NUMBER DIRECTION SET
C PLANE=0 (NODE ONLY, 1-3= X-Z, 4-6= LINE ALONG X-Z)
C DIRECTION= 0=ALL, 1-3= UX-UZ, 4-6= ANGX- ANGZ
NODE.NUMBER PLANE DIRECTION
C LEFT END OF PATCH
8           1     1
C CENTRE LINE OF PLATE
1           2     2
C END RESTRAINTS
C
SURFACE.FOR.PRESSURE
C LOAD.CASE PRESSURE.VALUE  START FINISH STEP  NODE PLANE
C AXIS  N1 N2 N3  LIST.OF.NODES
PRESSURE.VALUE NODE PLANE
C -100             13   2
C STRESS IN PLATE: ALL 3 ARE E/1000
-72.4              15   1
C STRESS IN PATCH
-207               17   1
C STRESS IN ADHESIVE
-1.89              34   1
-1.89              35   1
-1.89              36   1
C END PRESSURE
C
INCREMENTAL
C GAUSS.POINT.PRINT DISPLACEMENT.PRINT NODAL.STRESS.PRINT
C TIME.STEP STOP.TIME  MAX.STEP.NUMBER LOAD.CASE
C STEP.LIST
C *.PRINT= PRINT FREQ (DEF=3: 1,4,7,,,),
C TIME.STEP, STOP.T AND MAX.STEP.NUMBER = CREEP ONLY
C PARAMETERS, LOAD.CASE ?, STEP.LIST= SIZES OF LOAD
C INCREMENTS AS % OF TOTAL LOAD CASE(S- PAIRS ETC OF
C PROPORTIONS OF BASIS-SET LOADS)
STEP.LIST
100,10,10,10,10,10,10,10,10,10,10,10,10
C END INCREMENTAL
C
PLASTIC.MATERIAL
C PLASTIC.MATERIAL.NUMBER TYPE.OF.PLASTIC.MATERIAL
C PROPERTY.LIST
C PLAS.MAT. REFERRED BY YIELDING.ELEMENTS, TYPE.OF= 1 FOR
C ELASTIC (IN MATERIAL) AND POINT+ POST-YIELD SLOPES,
C 2= STRESS-STRAIN COORDS,
C PROP.LIST= CORRESPONDING DATA FOR TYPE.OF
C ******MANUAL APPEARS OUT OF DATE, NEED DIFFERENT
C HEADERS AS BELOW TO WORK
PLASTIC.MATERIAL YIELD.CRITERION UNIAXIAL.PROPERTIES
        12              1               1
```

```
C END PLASTIC.MATERIAL
UNIAXIAL.PLASTIC.PROPERTIES
UNIAXIAL TYPE PROPERTY.LIST
C *****note yield: shear=37MPa, von Mises=64.1
C    1       1    37,18.9
     1       1    64.1,18.9
C END UNIAXIAL.PLASTIC.PROPERTIES
C
YIELDING.ELEMENTS
C PLASTIC.MATERIAL.NUMBER CREEP.LAW.NUMBER  START FINISH
C STEP  GROUP.NUMBER LIST.OF.ELEMENTS
C PL.MAT REFERS TO PL.MAT.NO ABOVE (0= THAT OF EACH
C ELEMENT), CREEP FOR CREEP
C ONLY, REST= SPECIFYING PLASTIC ELEMENTS YIELDING
PLASTIC.MATERIAL.NUMBER  START FINISH STEP
          12              89    118    1
          12             439    474    1
          12             507    542    1
C END YIELDING.ELEMENTS
C
STATE.DETERMINATION
ALGORITHM
     1
C
END.OF.DATA
```

THIS PAGE INTENTIONALLY BLANK

Appendix C: Tables of Parameters from Cases Studied

File name	Value set	Calc β^1 (mm)	Stress β^1 (mm)	Fit β^1 (mm)	Calc F_Y/F_R (%)	Stress F_Y/F_R (%)	Fit F_Y/F_R (%)	Fit grad
Varying adhesive yield stress (Value in MPa)								
pl17	17.32	5.881	6.45	7.17	26.20	28.23	30.5	0.235
plong	37.00	5.881	6.40	8.17	55.96	60.3	67.0	0.122
plnew	**64.1**	**5.881**	**6.50**	**7.82**	**96.95**	**104.4**	**115**	**0.068**
pl100	100.0	5.881	6.40	7.70	151.25	163.0	179	0.043
Varying adhesive modulus								
e4	$E_A/4$	11.762	10.9	13.18	193.94	195.3	207	0.0637
e	$E_A/2$	8.317	8.95	9.60	137.14	146.5	150	0.064
2e	$2\ E_A$	4.159	4.85	6.14	68.58	72.4	89	0.069
4e	$4\ E_A$	2.941	3.45	4.34	48.49	49.6	70	0.062
Varying plate modulus								
ep2	$E_P/2$	4.740	5.41	7.10	156.32	162.2	200	0.0355
2ep	$2\ E_P$	6.883	7.43	8.26	56.75	60.6	63.5	0.130
Varying reinforcement modulus								
er2	$E_R/2$	4.867	5.50	6.57	80.25	87.65	98	0.067
2er	$2\ E_R$	6.704	7.45	8.58	110.54	116.6	128	0.067
Varying adhesive thickness								
t	$2t_A$	8.317	8.85	10.12	137.14	138.85	151	0.067

C.1. Notes to, and definitions of terms in, the above table.

The row in bold is the "base case": all parameters were varied from this case as indicated.

Calc: calculated using configuration and one dimensional model formulae.

stress: obtained from σ_{xy} stress data (Figure 5, 7).

Fit: linear fit to plastic zone growth plot (Figure 9).

β^1 (mm): Load transfer length in mm

F_Y/F_R (%): yield load as a percentage of the reference load (far field $E/1000$ stresses applied: Figure 2).

Fit grad: gradient of the linear fit to the plot of plastic zone length in mm, against applied load.

DISTRIBUTION LIST

Finite Element Analysis of the Double Lap Joint with an Elastic-Plastic Adhesive

C. Pickthall, M. Heller and L.R.F. Rose

AUSTRALIA

DEFENCE ORGANISATION

Task sponsor AIR OIC ASI-LSA

S&T Program

Chief Defence Scientist
FAS Science Policy
AS Science Corporate Management
} shared copy

Director General Science Policy Development
Counsellor Defence Science, London (Doc Data Sheet only)
Counsellor Defence Science, Washington (Doc Data Sheet only)
Director General Scientific Advisers and Trials and Scientific Adviser Policy and Command (shared copy)
Navy Scientific Adviser (Doc Data Sheet and distribution list only)
Scientific Adviser - Army (Doc Data Sheet and distribution list only)
Air Force Scientific Adviser
Director Trials

Aeronautical and Maritime Research Laboratory

Director
Chief of Airframes and Engines Division
Research Leader Fracture Mechanics
Research Leader Aerospace Structures
C. Pickthall (5 copies)
M. Heller (5 copies)
L.R.F. Rose
R.J. Chester
R.J. Callinan
P. Chalkey

DSTO Library

Library Fishermens Bend
Library Maribyrnong
Library Salisbury (2 copies)
Australian Archives
Library, MOD, Pyrmont (Doc Data sheet only)

Capability Development Division

Director General Maritime Development (Doc Data Sheet only)
Director General Land Development (Doc Data Sheet only)
Director General C3I Development (Doc Data Sheet only)

Army
ABCA Office, G-1-34, Russell Offices, Canberra (4 copies)

Intelligence Program
DGSTA Defence Intelligence Organisation
Library, Defence Signals Directorate (Doc Data Sheet only)

Corporate Support Program (libraries)
OIC TRS, Defence Regional Library, Canberra
Officer in Charge, Document Exchange Centre (DEC), 1 copy
*US Defence Technical Information Center, 2 copies
*UK Defence Research Information Centre, 2 copies
*Canada Defence Scientific Information Service, 1 copy
*NZ Defence Information Centre, 1 copy
National Library of Australia, 1 copy

UNIVERSITIES AND COLLEGES

Australian Defence Force Academy
Library
Head of Aerospace and Mechanical Engineering
Deakin University, Serials Section (M list), Deakin University Library, Geelong, 3217
Senior Librarian, Hargrave Library, Monash University
Librarian, Flinders University

OTHER ORGANISATIONS

NASA (Canberra)
AGPS

OUTSIDE AUSTRALIA

ABSTRACTING AND INFORMATION ORGANISATIONS
INSPEC: Acquisitions Section Institution of Electrical Engineers
Library, Chemical Abstracts Reference Service
Engineering Societies Library, US
Materials Information, Cambridge Scientific Abstracts, US
Documents Librarian, The Center for Research Libraries, US

INFORMATION EXCHANGE AGREEMENT PARTNERS
Acquisitions Unit, Science Reference and Information Service, UK
Library - Exchange Desk, National Institute of Standards and Technology, US

SPARES (10 copies)

Total number of copies: 67

DEFENCE SCIENCE AND TECHNOLOGY ORGANISATION
DOCUMENT CONTROL DATA

1. PRIVACY MARKING/CAVEAT (OF DOCUMENT)

2. TITLE

Finite Element Analysis of the Double Lap Joint with an Elastic-Plastic Adhesive

3. SECURITY CLASSIFICATION (FOR UNCLASSIFIED REPORTS THAT ARE LIMITED RELEASE USE (L) NEXT TO DOCUMENT CLASSIFICATION)

Document (U)
Title (U)
Abstract (U)

4. AUTHOR(S)

C. Pickthall, M. Heller and L.R.F. Rose

5. CORPORATE AUTHOR

Aeronautical and Maritime Research Laboratory
PO Box 4331
Melbourne Vic 3001

6a. DSTO NUMBER	6b. AR NUMBER	6c. TYPE OF REPORT	7. DOCUMENT DATE
DSTO-TR-0528	AR-010-216	Technical Report	May 1997

8. FILE NUMBER	9. TASK NUMBER	10. TASK SPONSOR	11. NO. OF PAGES	12. NO. OF REFERENCES
M1/9/112	95/228	AIR OIC ASI-LSA	23	4

13. DOWNGRADING/DELIMITING INSTRUCTIONS

None

14. RELEASE AUTHORITY

Chief, Airframes and Engines Division

15. SECONDARY RELEASE STATEMENT OF THIS DOCUMENT

Approved for public release

OVERSEAS ENQUIRIES OUTSIDE STATED LIMITATIONS SHOULD BE REFERRED THROUGH DOCUMENT EXCHANGE CENTRE, DIS NETWORK OFFICE, DEPT OF DEFENCE, CAMPBELL PARK OFFICES, CANBERRA ACT 2600

16. DELIBERATE ANNOUNCEMENT

No Limitations

17. CASUAL ANNOUNCEMENT Yes

18. DEFTEST DESCRIPTORS

finite element analysis, adhesive bonding, lap joints, yield strength

19. ABSTRACT

For an effective adhesively bonded reinforcement of a (typically cracked) plate, sufficient load must be transferred by the adhesive into the reinforcement to prevent the underlying damage from growing. Under severe load, the adhesive may yield plastically. Notwithstanding possible adhesive failure, this may be beneficial to the reinforcement by reducing the peak stress adjacent to the crack. In this paper, characterisation of this stress reduction compared to the (non-yielding) elastic case, was sought by examining the influences of configurational parameters including plate, adhesive and reinforcement moduli, and adhesive yield stress. Finite element (FE) analyses were conducted for a two-dimensional section through a double-sided (symmetric) lap joint, representative of a typical repair. Stress reductions in the reinforcement of the order of 25% were found. The adhesive yield was shown to be dominated by shear stress, and thus the adhesive behaved essentially one-dimensionally. The linear increase in plastic zone length with applied load, as predicted by the Hart-Smith one-dimensional theory, was in good agreement with the FE results. However the observed load transfer length was 6-18% longer than predicted.